Supplementary material for the paper **ADSO-D-12-00179** in ***Adsorption*** journal

(paper's **DOI**: 10.1007/s10450-012-9462-7)

"Adsorption and desorption kinetics of benzene derivatives on mesoporous carbons"

by **Adam W. Marczewski*, Anna Derylo-Marczewska** and Agata Slota**

*e-mail: Adam.Marczewski@umcs.lublin.pl , ** e-mail: annad@hektor.umcs.lublin.pl

*Dept. www: http://Radiochemistry.umcs.lublin.pl personal www: http://guide.adsorption.org

** Dept. www: http://SurfaceSci.umcs.lublin.pl

Contents

Appendix for the Theory - Flying start approach to solving kinetic equations

If we know a solution (or some numerical procedure) of some kinetic equation at specific initial conditions (c_x, θ_x) and the rate depends only on the temporary state of such system (e.g. for Langmuir and SRT kinetics involving lateral interactions and energetic heterogeneity but not intraparticle diffusion model) we may easily find more general solutions by using a simple general geometric scheme called here the *flying start* approach. The initial conditions (c_o, θ_o) of a given adsorption system may be treated as a temporary state of some imaginary kinetics with the initial conditions (c_x, θ_x) and the same equilibrium (c_{eq}, θ_{eq}). It means that in the coordinates of this imaginary kinetics, (c_o, θ_o) are flying start conditions of our real experiment and we should extrapolate conditions backwards to (c_x, θ_x) (see Fig. 1 for adsorption scheme).

At our flying start, i.e. initial conditions of the real experiment (c_o, θ_o), the adsorption progress of the imaginary kinetics F' is F_o and $F' = F_o + F(1 - F_o)$. However, time of the real experiment t is $t(F) = t'(F') - t'(F_o)$ where $t'(F')$ is the time of the imaginary kinetics. For adsorption with θ_x=0

(e.g. IKL) we have $F_o=\theta_o/\theta_{eq}$ and $c_x=(c_o\theta_{eq}-c_{eq}\theta_o)/(\theta_{eq}-\theta_o)$. For desorption with c_x=0 (e.g. dIKL) we obtain $F_o=c_o/c_{eq}$ and $\theta_x=(c_{eq}\theta_o-c_o\theta_{eq})/(c_{eq}-c_o)$. In general this technique may be used for any kinetics with the rate which depends only on the temporary state of the system.

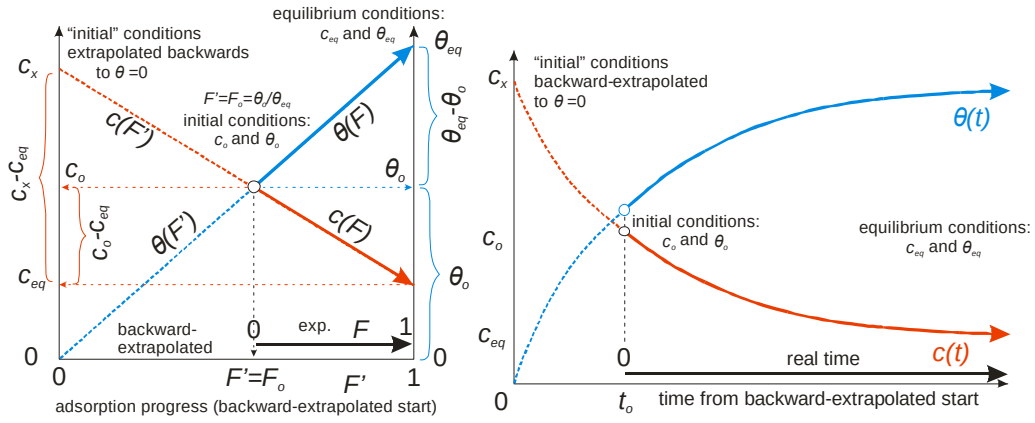

Fig. S1. The idea and calculation scheme of the *flying-start* kinetic approach to **adsorption kinetics** with some pre-adsorbed solute. Initial conditions: (c_o, θ_o), equilibrium: (c_{eq}, θ_{eq}). F – adsorption progress, F' - adsorption progress of the imaginary experiment with the same equilibrium (c_{eq}, θ_{eq}) and temporary (c_o, θ_o) conditions.

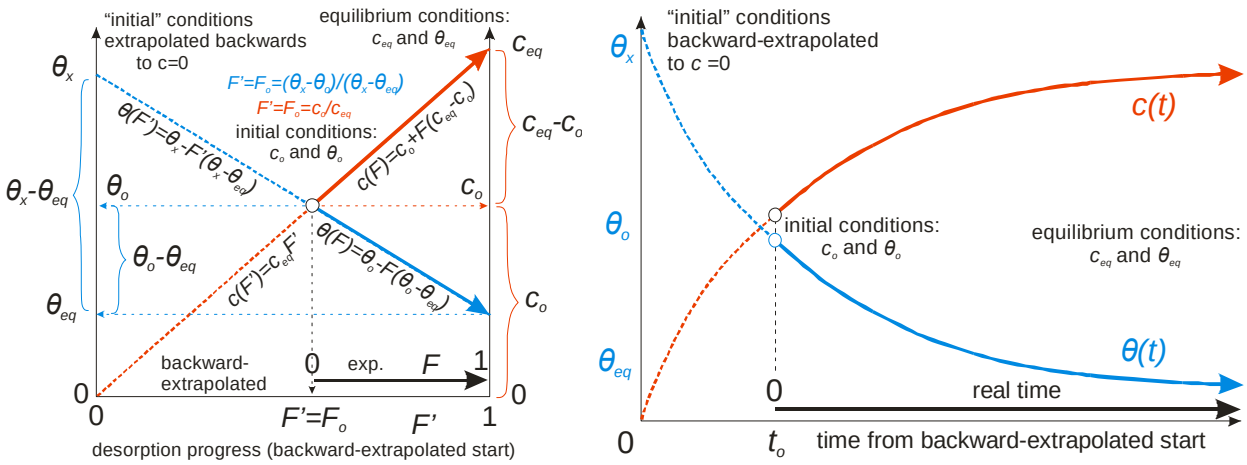

Fig. S2. The idea and calculation scheme of the *flying-start* kinetic approach to **desorption kinetics** with non-zero initial solute concentration. Initial conditions: (c_o, θ_o), equilibrium: (c_{eq}, θ_{eq}). F – desorption progress, F' - desorption progress of the imaginary experiment with the same equilibrium (c_{eq}, θ_{eq}) and temporary (c_o, θ_o) conditions.

By using this method we may generalize simpler equations (e.g. IKL and dIKL to gIKL) with much less effort than is required for analytical solution from scratch. Moreover, in the case of IKL and dIKL the obtained equations are of the same type as the basic equations for standard initial conditions (IKL for zero coverage, θ_o =0 and dIKL for zero concentration, c_o=0). However, the Langmuir batch equilibrium factor f_L of such a kinetic "fragment" is always smaller in magnitude $|f_L|$ than the value f_x for the imaginary kinetics which it is part of, $f_L=f_x(1-F_o)/(1-f_xF_o)$. The only exceptions are the second order adsorption kinetics ($f_L=f_x=1$) and first order adsorption or

desorption kinetics ($f_L = f_x = 0$) which do not change behavior if the initial conditions (θ_o for adsorption or c_o for desorption) are changed.

Theory - supplementary figures

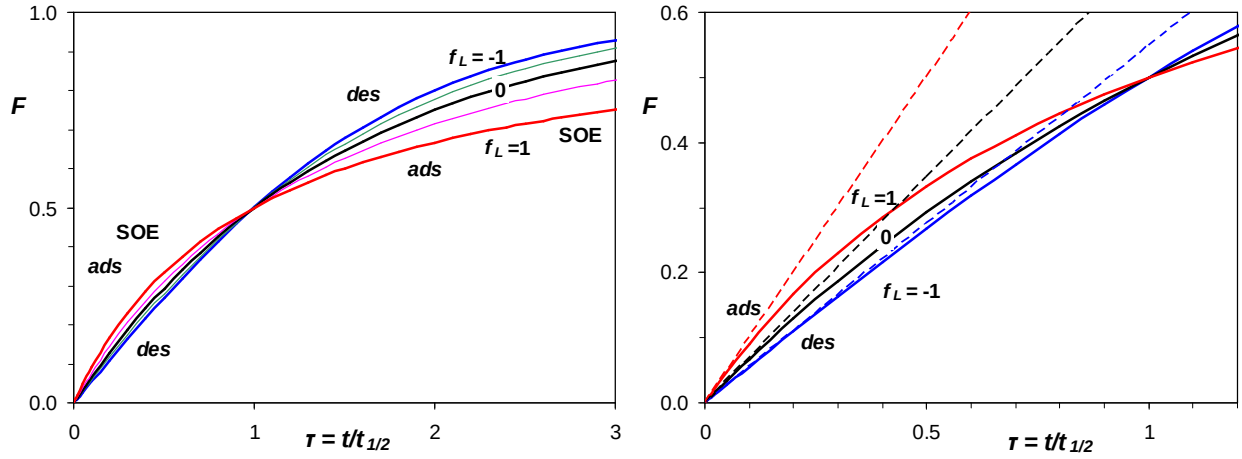

Fig. S3. Adsorption progress, F, vs. reduced time, $\tau=t/t_{1/2}$ for gIKL Eq. (6) (f_L changes from -1 to 1 with 0.5 step). The dashed lines correspond to the initial rates (right).

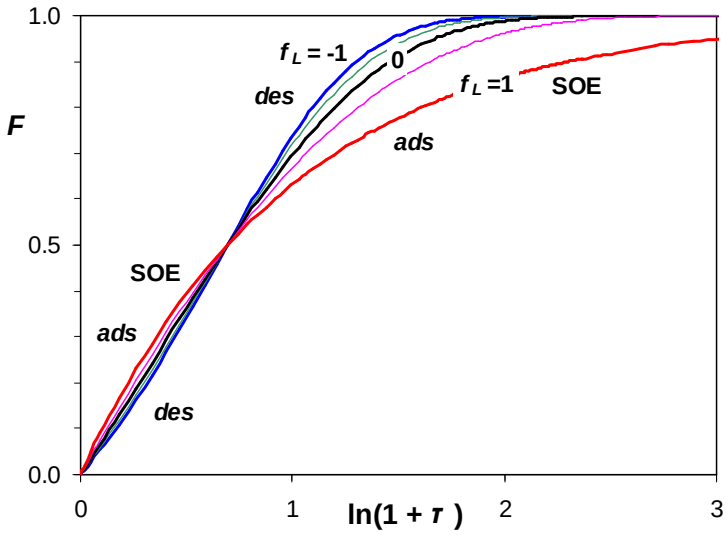

Fig. S4. Adsorption progress, F, vs. half-log reduced time scale, ln(1+τ), where $\tau=t/t_{1/2}$ for gIKL Eq. (6); f_L changes from -1 to 1 with 0.5 step.

Results and discussion - supplementary figures, tables and analyses

Synthesis

Synthesis and adsorption data were partly discussed in:

Derylo-Marczewska, A.; Marczewski, A.W.; Slota, A.: Kinetics of adsorption and desorption for selected organics from aqueous solutions on mesoporous solids. Proc. 12th Polish-Ukrainian Symp. on Theoretical and Experimental Studies

of Interfacial Phenomena and Their Technological Applications (TESIP-12), ISBN 978-83-227-3180-2, Ameliówka (Kielce), Poland, Aug 24-28, 2010, p.26 (only 1 page abstract).

Synthesis – modification of the original methods (silica synthesis: Zhao et al. 1998; direct carbon synthesis: Kim et al. 2004) - see details below.

Carbon synthesis details:

Polymer1 (for W84,W87)– Pluronic PE6400 (from BASF) - non-ionic copolymer $(EO)_{13}(PO)_{30}(EO)_{13}$, where EO-ethylene oxide, PO-propylene oxide (M = 2900 g/mol)
Polymer2 (for W85) – Pluronic PE9400 (from BASF) - non-ionic copolymer $(EO)_{21}(PO)_{47}(EO)_{21}$ (M = 4600 g/mol)

TEOS – tetraethylorthosilicate, PhTEOS – phenyl-triethylortosilicate
TMB - 1,3,5-trimethylbenzene

1. Silicas: Dissolve 10 g of polymer in 360 ml of 1.6M HCl, add 10 g of TMB, stir slowly at 35°C for 45 min, add 28 g TEOS and 6 g of PhTEOS, keep stirring for 20 hrs, put in autoclave at 70°C-120°C for 24 hrs, cool down, put on fine filtrating paper and rinse with distilled water. Autoclave temperatures: 70°C (for W84), 120°C (W85), 100°C (W87) were selected to obtain divergent silica and carbon properties

2. Carbonization: carbon-silica composite from as-synthesized silica (direct method): Add 4 g of water and 0.08 g of H_2SO_4 per 1 g of as-synthesized silica, mix for 30 min, put into vacuum dryer for 12 hrs at 100°C, then keep at 160°C for 12 hrs. Continue carbonization at 800°C in nitrogen atmosphere for 6 hrs.

3. Etching: carbon from carbon-silica composite: KOH or NaOH in 50:50 EtOH/water solution

Typically only 2 g of carbon is obtained from the initial 10 g of polymer.

Isotherm data

Adsorption of SA is always much stronger than adsorption of BA and adsorption of BA is stronger than adsorption of Ph.

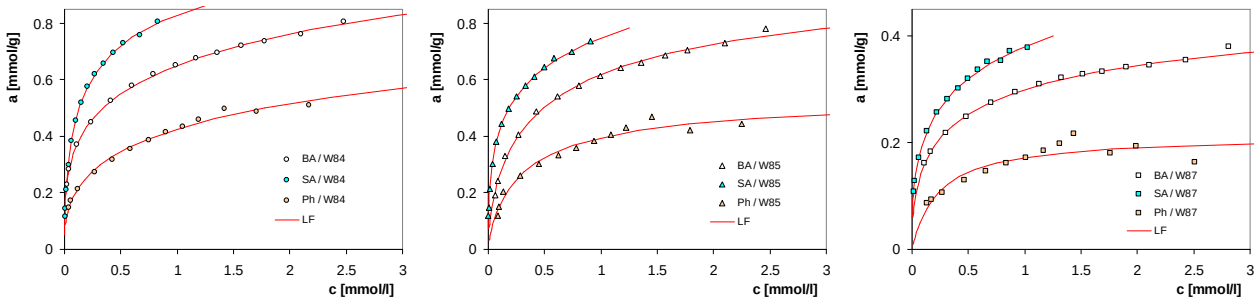

Fig. S5. Equilibrium adsorption isotherms of BA, SA and Ph on carbons W84 (left), W85 (middle) and W87 (right) – comparison of adsorbate effects (see also Fig. 8 in the paper).

Kinetic data:

All initial concentrations (BA, SA, Ph) were the same (2.2 mmol/l, pH=2). Adsorbent to solution proportion was 50 mg / 50 ml (i.e. 1 g/L) . All concentrations were determined by using entire UV

spectra (200-400 nm). Solution was collected cyclically from the Erlenmeyer flask by using the 10 mm quartz flow cell, PTFE tubing with inlet equipped with a glass wool filter (3 mm diameter, 5 mm length) and peristaltic pump (cycle times increased during measurements) with the solution returning to the reaction vessel after spectrum registration. After prescribed time (7-24 hrs), when adsorption equilibrium was near enough, 1 ml of 1M NaOH was added to force desorption (earlier experiments for various carbon materials showed that adsorption of organic aromatic acids – BA, SA, Ph - is the strongest for their molecular forms (pH << pK_a) and the weakest for their anionic forms (pH >> pK_a)). Then desorption was recorded in the same way as adsorption.

Note. *Glass wool filter is required to prevent entrance of small particulate matter into the flow cell (filter may be skipped for commercial sorbent with hard durable adsorbent particles), however, its use may cause creation of air bubbles in the tubing and flow cell (peristaltic pump sucks solution through this filter and flow cell) or even blocking the tubing (excess of small particulate matter).*

For example for BA on W85 carbon, m=0.0515 g, 50 ml of BA solution (pH=2); alkalization: 1ml of 1M NaOH added after 440 min from start of adsorption kinetics

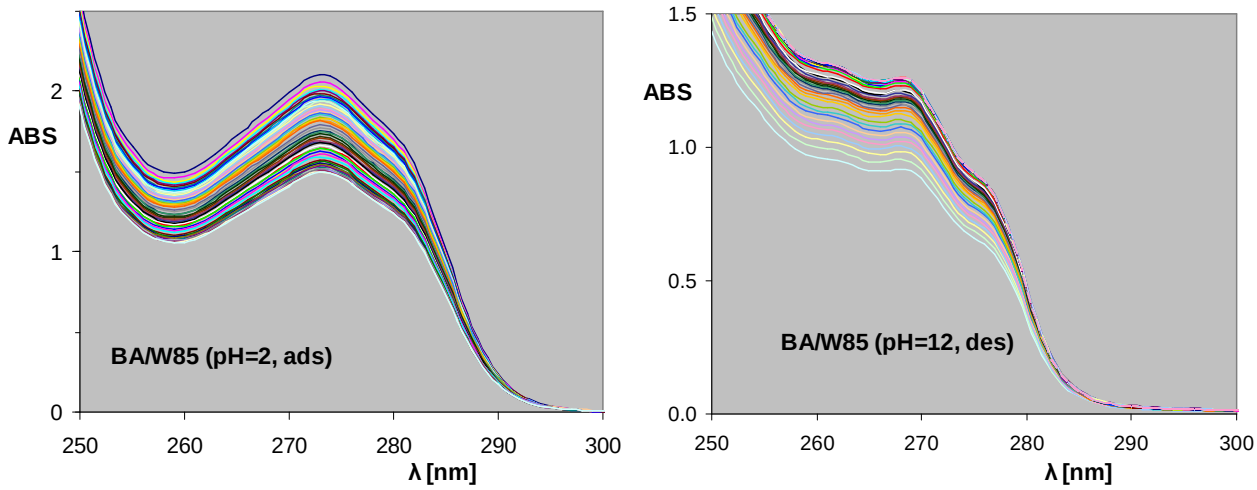

Fig. S6. UV/Vis absorption data (fragment) for adsorption and desorption BA/W85 kinetic experiments (after background correction).

See below comparison of adsorption isotherm of BA on W85 with the kinetic operating line.

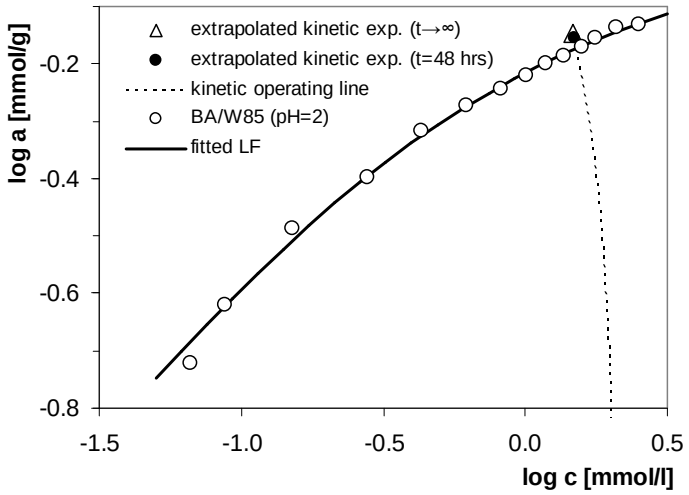

Fig. S7. Equilibrium adsorption isotherm of BA on carbon W85 (open circles). Thick solid line is the Langmuir-Freundlich fit. The kinetic operating line (dotted curve), extrapolated equilibrium point (white triangle) and extrapolated adsorption after 48 hrs (black circle) are shown for comparison.

Preliminary kinetic analysis - Bangham plots

Aharoni, C., Sideman, S., Hoffer, E.: Adsorption of phosphate ions by collodion-coated alumina. J. Chem. Technol. Biotechnol. **29**, 404-412 (1979).

Linear plots in Bangham coordinates log(log($c_o/_c$)) vs. log t correspond to Avrami (or KEKAM) kinetic equation that may be represented as adsorbate uptake $u(t) = 1 - \exp[-(kt)^p]$. However, actual data shows only partial linearity in Bangham coordinates. Figure shows influence of adsorbate on adsorption kinetics: adsorbate uptake is always the fastest for SA. Uptake of BA is slower but not much slower, however, uptake of phenol is always lower and this difference is much more pronounced for longer times.

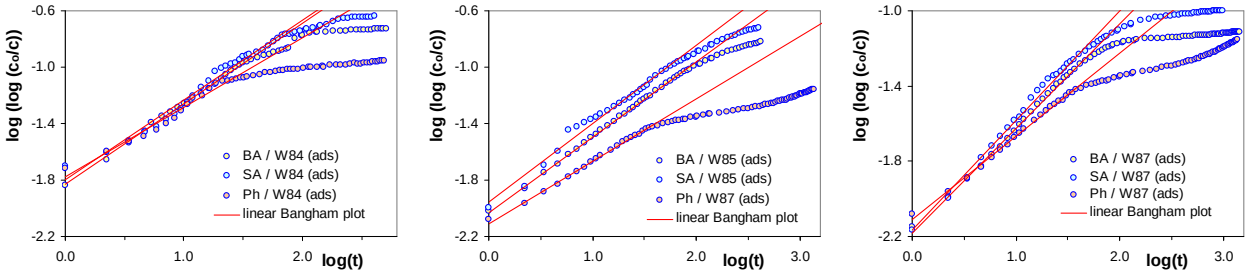

Fig. S8. Bangham plots: comparison of adsorbate effect.

Parameter values are also compared in Table 1 and 2. For all adsorbates rate coefficient, k, as well power coefficient, n, decrease regularly in the series W84, W85 and W87 (Table 1). Moreover, rate coefficients for SA are always the largest, while for phenol are the smallest if adsorption data is compared for any single carbon material (Table 2). The same is true for parameter n (only for BA and SA on W84 parameters are practically equal).

Table S1. Parameters of linear part of Bangham plots: effect of carbon type.

Adsorbate / parameter	**Carbons / parameter values**		
BA	**W84**	**W85**	**W87**
k	0.00263	0.00076	0.00054
p	0.569	0.535	0.556
SA	**W84**	**W85**	**W87**
k	0.00287	0.00134	0.00079
p	0.566	0.556	0.581
Ph	**W84**	**W85**	**W87**
k	0.00133	0.00028	0.00011
p	0.492	0.465	0.442

Table S2. Parameters of linear part of Bangham plots: effect of adsorbate type.

Carbon / parameter	**Adsorbate / parameter values**		
W84	**BA**	**SA**	**Ph**
k	0.00263	0.00287	0.00133
p	0.569	0.566	0.492
W85	**BA**	**SA**	**Ph**
k	0.00076	0.00134	0.00028
p	0.535	0.556	0.465
W87	**BA**	**SA**	**Ph**
k	0.00054	0.00079	0.00011

p	0.556	0.581	0.442

Intraparticle diffusion model, IDM (Crank 1954).

Crank, J.: Mathematics of Diffusion. Oxford University Press, London (1954):

Intraparticle diffusion with varying concentration (u_{eq}=1-c_{eq}/c_o) and spherical sorbent particles.

Optimized parameters: c_o, D_a/r^2, c_{eq} (middle part of the Table below)

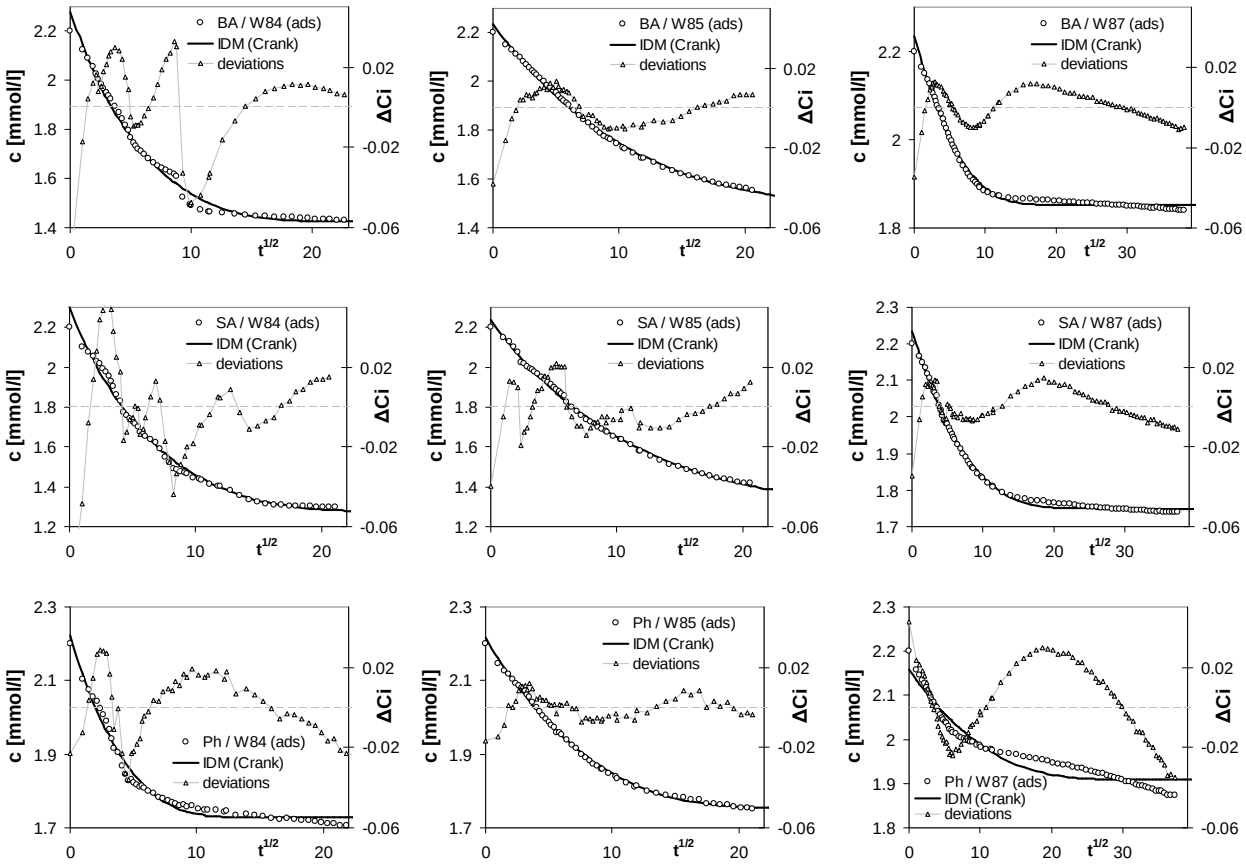

Fig. S9. Adsorption (pH=2) data of BA, SA and Ph on mesoporous carbons W84, W85, W87 compared with intraparticle diffusion model (Crank 1954). Deviations are indicated. Time is in [min].

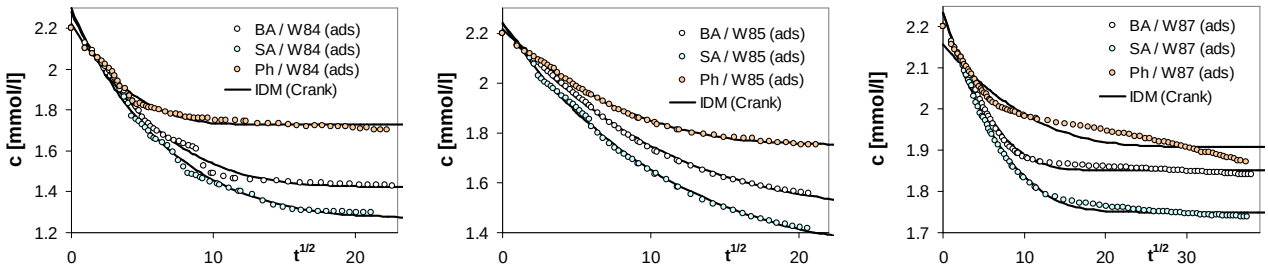

Fig. S10. Adsorption (pH=2) data of BA, SA and Ph on mesoporous carbons W84, W85, W87 - effect of adsorbate. Lines are fitted to the intraparticle diffusion model (Crank 1954). Time is in [min].

For a model ideally suitable for the experimental data, fitting method should not have great impact on the parameters. However, by turning on and off optimization of critical parameters, we may observe whether this model in this critical areas well describes our data. Especially, when we know some parameter from the experiment (here, experimental initial concentration, c_{ini} should be the

same as obtained from optimization, c_o). Thus 3 kinds of optimizations presented in Table S3 try to answer if IDM suits well the data. First we use experimental c_o=c_{ini} and u_{eq} is calculated from u_{eq}=(1-c_{eq}/c_o). Then we allow c_o to be adjusted and strong improvement of fitting quality suggests that the initial part of kinetics is not very well described by the model. Finally, we allow u_{eq} to be optimized independently of c_o and c_{eq}. Again large improvement of *SD* and R^2 makes it obvious, that the actual effect of change of concentration in solution on sorption kinetics is much weaker that predicted by the IDM (u_{eq}<<(1-c_{eq}/c_o) - the only discrepancy is observed for Ph/W87) the . It may be attributed to strong adsorption-driven accumulation of adsorbate in external parts of granules where the desorption for adsorbate-saturated surface as the source of adsorbate for further pore penetration is much more stable then the variable solution concentration thus stabilizing the rate (adsorption rate-controlling mechanism).

Table S3. Effect of fitting assumptions on optimized parameters and fitting quality (IDM). Units: c_o, c_{eq}, *SD*(*c*) [mmol/l], D/r^2 [min^{-1}], d*c*/d($t^{1/2}$) [mmol/l $min^{-0.5}$], D_a [cm^2/s], halftime t_{05} [min].

BA	**W84**	**W85**	**W87**	**W84**	**W85**	**W87**	**W84**	**W85**	**W87**
fitting	**c_{eq}, D/r^2**			**c_o, c_{eq}, D/r^2**			**c_o, c_{eq}, D/r^2, u_{eq}**		
c_o	2.2	2.2	2.2	2.279	2.238	2.235	2.252	2.224	2.228
c_{eq}	1.413	1.449	1.85	1.423	1.502	1.851	1.432	1.542	1.851
D/r^2	0.00077	0.00026	0.00131	0.00098	0.00039	0.00154	0.00179	0.00076	0.00189
u_{eq}	0.358	0.342	0.159	0.376	0.329	0.172	0	0	0
SD(c)	0.0335	0.0148	0.0113	0.0246	0.0095	0.0084	0.0153	0.0059	0.0076
1-R^2	0.01601	0.00585	0.01292	0.0086	0.00243	0.0072	0.00333	0.00094	0.00583
dc/d($t^{1/2}$)$_{ini}$	0.01007	0.00546	0.00445	0.01269	0.00638	0.00536	0.01025	0.00554	0.00484
D_a x 10^9	**2.9**	**0.99**	**4.9**	3.68	1.46	5.76	6.72	2.83	7.1
t_{05}	20.33	62.21	18.14	15.32	43	15.1	17.05	40.44	16.14
SA	**W84**	**W85**	**W87**	**W84**	**W85**	**W87**	**W84**	**W85**	**W87**
fitting	**c_{eq}, D/r^2**			**c_o, c_{eq}, D/r^2**			**c_o, c_{eq}, D/r^2, u_{eq}**		
c_o	2.2	2.2	2.2	2.299	2.24	2.234	2.256	2.219	2.226
c_{eq}	1.239	1.253	1.748	1.273	1.325	1.75	1.302	1.397	1.75
D/r^2	0.00048	0.00019	0.00084	0.00066	0.00029	0.00097	0.00146	0.00073	0.00122
u_{eq}	0.437	0.43	0.206	0.446	0.408	0.217	0	0	0.049
SD(c)	0.0377	0.0169	0.0117	0.0274	0.0125	0.0085	0.021	0.0096	0.0084
1-R^2	0.01897	0.00531	0.00738	0.01004	0.00288	0.00394	0.00588	0.0017	0.00378
dc/d($t^{1/2}$)$_{ini}$	0.01104	0.00678	0.00487	0.01407	0.00779	0.00571	0.01076	0.00658	0.00516
D_a x 10^9	**1.8**	**0.71**	**3.15**	2.48	1.09	3.65	5.46	2.75	4.58
t_{05}	26.62	68.27	25.94	18.83	47	21.89	20.97	41.6	23.28
Ph	**W84**	**W85**	**W87**	**W84**	**W85**	**W87**	**W84**	**W85**	**W87**
fitting	**c_{eq}, D/r^2**			**c_o, c_{eq}, D/r^2**			**c_o, c_{eq}, D/r^2, u_{eq}**		
c_o	2.2	2.2	2.2	2.223	2.217	2.157	2.214	2.208	2.199
c_{eq}	1.726	1.747	1.915	1.727	1.752	1.908	1.729	1.757	1.857
D/r^2	0.00265	0.00077	0.00099	0.00286	0.00086	0.00058	0.00387	0.00116	$4.6\cdot10^{-8}$
u_{eq}	0.216	0.206	0.129	0.223	0.21	0.116	0	0	0.995
SD(c)	0.0174	0.0079	0.0211	0.0167	0.0062	0.0194	0.0166	0.0051	0.0119
1-R^2	0.02002	0.00366	0.06918	0.01858	0.00227	0.05835	0.01818	0.00153	0.02216
dc/d($t^{1/2}$)$_{ini}$	0.00919	0.00468	0.00304	0.01009	0.00509	0.00201	0.00890	0.00454	0.00407
D_a x 10^9	**9.93**	**2.88**	**3.72**	10.74	3.21	2.19	14.49	4.34	0.000173
t_{05}	8.07	28.3	25.17	7.35	25	43.86	7.9	26.39	40.21

If we look at the initial dc/d$t^{1/2}$ slopes calculated as: $(c_o - c_{eq})(\pi D / r^2)^{1/2} / [6(1-u_{eq})]$) (see Table), we may see that they are similar enough for different optimization approaches. However, this would

be much different if we would use $c_o u_{eq}(\pi D/r^2)^{1/2}/[6(1-u_{eq})]$ instead (should be its equivalent, as results from IDM model assumptions), but due to the "unconnected" c_{eq} and u_{eq} in the last of optimization types we have $c_o u_{eq} \neq (c_o - c_{eq})$.

For effective diffusion coefficients D_a calculated from Table above, by assuming that $c_o = c_{ini}$ and uptake in agreement with c_o and c_{eq} (i.e. $u_{eq} = 1 - c_o/c_{eq}$):

Comparison of effective diffusion coefficients (**carbon effect**):

BA (W84, W85, W87): $D_a = 2.9 \cdot 10^{-9}$, $0.98 \cdot 10^{-9}$, $4.9 \cdot 10^{-9}$ cm^2/s

SA (W84, W85, W87): $D_a = 1.8 \cdot 10^{-9}$, $0.71 \cdot 10^{-9}$, $3.1 \cdot 10^{-9}$ cm^2/s

Ph (W84, W85, W87): $D_a = 9.9 \cdot 10^{-9}$, $2.9 \cdot 10^{-9}$, $3.7 \cdot 10^{-9}$ cm^2/s

Comparison of effective diffusion coefficients (**adsorbate effect**):

W84 (BA, SA, Ph): $D_a = 2.9 \cdot 10^{-9}$, $1.8 \cdot 10^{-9}$, $9.9 \cdot 10^{-9}$ cm^2/s,

W85 (BA, SA, Ph): $D_a = 0.98 \cdot 10^{-9}$, $0.71 \cdot 10^{-9}$, $2.9 \cdot 10^{-9}$ cm^2/s

W87 (BA, SA, Ph): $D_a = 4.9 \cdot 10^{-9}$, $3.1 \cdot 10^{-9}$, $3.7 \cdot 10^{-9}$ cm^2/s

If we look at kinetic halftimes (for optimized c_o), we may see that the slowest kinetics is on W85 (geometric average for all adsorbates, t_{05}=37 min), whereas for W84 it is the fastest (13 min) and for W87 is in between (24 min). Thus the effect of micropore presence and average pore size are evident.

IDM, optimized: c_{eq}, D/r^2

t_{05} [min]	W84	W85	W87	geom.avg
BA	20.33	62.21	18.14	28.41
SA	26.62	68.27	25.94	36.12
Ph	8.07	28.3	25.17	17.92
geom.avg	16.35	49.35	22.79	26.39

IDM, optimized: c_o, c_{eq}, D/r^2

t_{05} [min]	W84	W85	W87	geom.avg
BA	15.32	43.35	15.1	21.56
SA	18.83	47.43	21.89	26.94
Ph	7.35	25.24	43.86	20.12
geom.avg	12.85	37.3	24.38	22.69

IDM, optimized: c_o, c_{eq}, D/r^2, u_{eq}

t_{05} [min]	W84	W85	W87	geom.avg
BA	17.05	40.44	16.14	22.32
SA	20.97	41.6	23.28	27.28
Ph	7.9	26.39	40.21	20.32
geom.avg	14.14	35.41	24.72	23.13

Pore diffusion model, PDM (Mc Kay 1996)

McKay, G., El Geundi, M., Nassar, M.M.: Pore diffusion during the adsorption of dyes onto bagasse pith. Proc. Safety Environ. Prot. 74, 277-288 (1996); (see also Castillejos et al. 2011)**:**

McKay's pore diffusion model assuming unreacted shrinking core and including external film transfer resistance:

Capacity factor: $C_h = u_{eq} = (c_o\text{-}c_{eq})/c_o$, B=1-1/Bi, where Biot number $Bi=K_f r/D_p$ – (D_p – pore diffusion coefficient, r – particle radius, K_f - external mass transfer coefficient),

dimensionless time in McKay's pore diffusion model τ_s:

$$\tau_s = \frac{1}{6C_h}\left\{\left(2B-\frac{1}{a}\right)\ln\left[\left|\frac{x^3+a^3}{1+a^3}\right|\right]+\frac{3}{a}\ln\left[\left|\frac{x+a}{1+a}\right|\right]\right\}+\frac{1}{a\sqrt{3}C_h}\left\{\arctan\left(\frac{2-a}{a\sqrt{3}}\right)-\arctan\left(\frac{2x-a}{a\sqrt{3}}\right)\right\}$$

where $x=(1-F)^{1/3}$, $a=(1/C_h-1)^{1/3}$, then $x^3+a^3=1/C_h-F$ and $1+a^3=1/C_h$ and rate:

$$\frac{dF}{d\tau_s}=\frac{3(1-C_hF)(1-F)^{1/3}}{1-B(1-F)^{1/3}}$$

The reduced experiment time, may be then calculated as $\tau = t/t_{1/2} = \tau_s/\tau_{s1/2}$, where ½ index denotes value at F=0.5 and $t(F)=\tau_s(F)/\tau_s(0.5)t_{1/2}$.

Statistically, the deviations from McKay's model are the smallest if the entire data set is considered (McKay < MOE < Crank), especially near the beginning (if all exp. points are included, McKay's model is only slightly worse that MOE without 2 initial points). However, while for Crank and MOE models deviations become smaller near the equilibrium, deviations from this pore diffusion model are growing and trends of experimental data and fitted lines become divergent and it is likely that if the experiment were longer, the discrepancies between McKay's model and data would grow, unless new optimization were performed. In this respect MOE and Crank models seem to follow near-equilibrium data more closely. This problem with McKay's model seems to be related to the approximations of the shrinking core approach (leading to the equilibrium after some finite time, $\tau_{s,eq}=\tau_s(F=1,B,Ch)$).

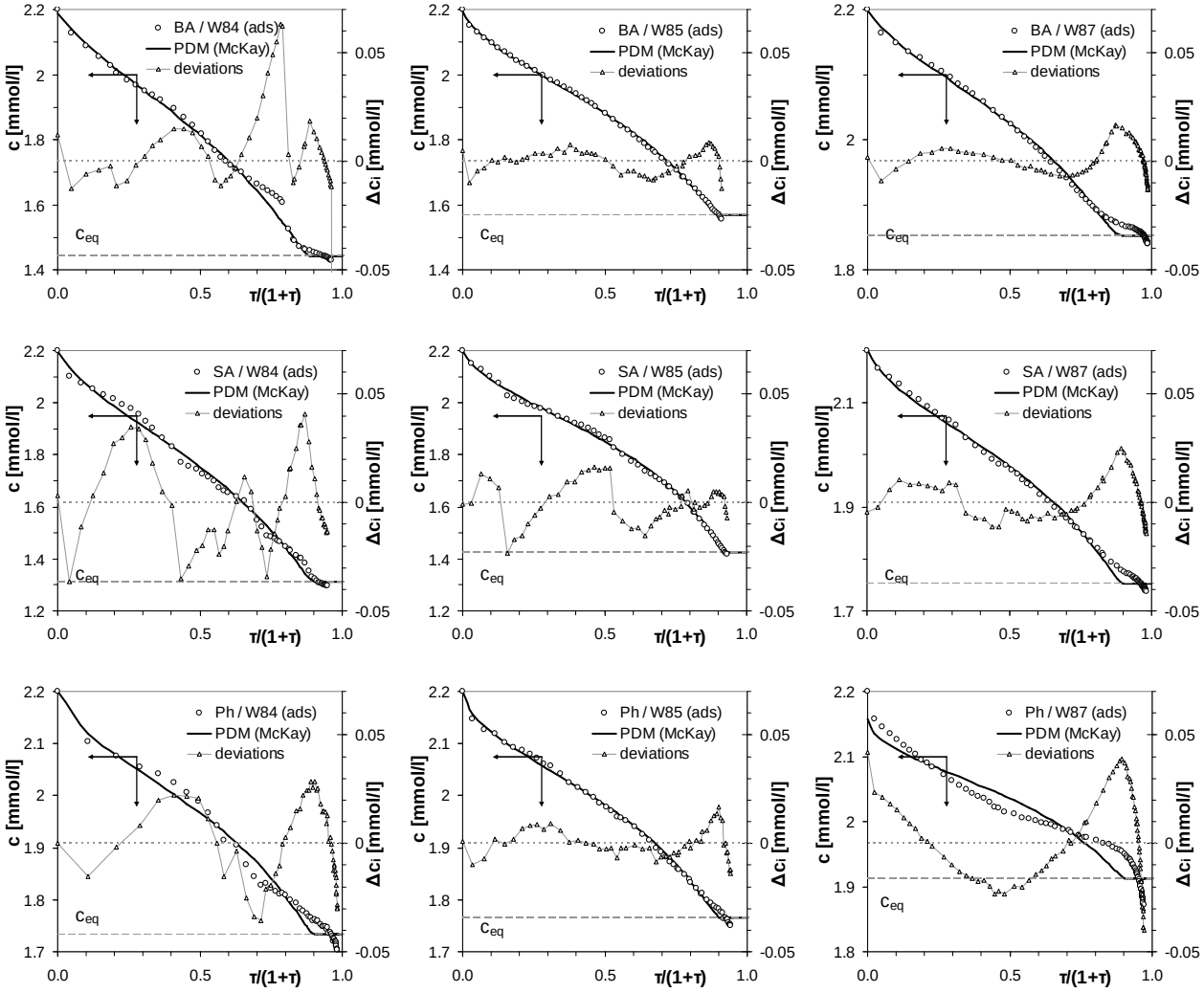

Fig. S11. Adsorption (pH=2) data of BA, SA and Ph on mesoporous carbons W84, W85, W87 in compact time plot, concentration vs. $\tau/(1+\tau)$, where $\tau = t/t_{0.5}$ is reduced time. Solid lines are PDM-optimizations. Deviations are indicated.

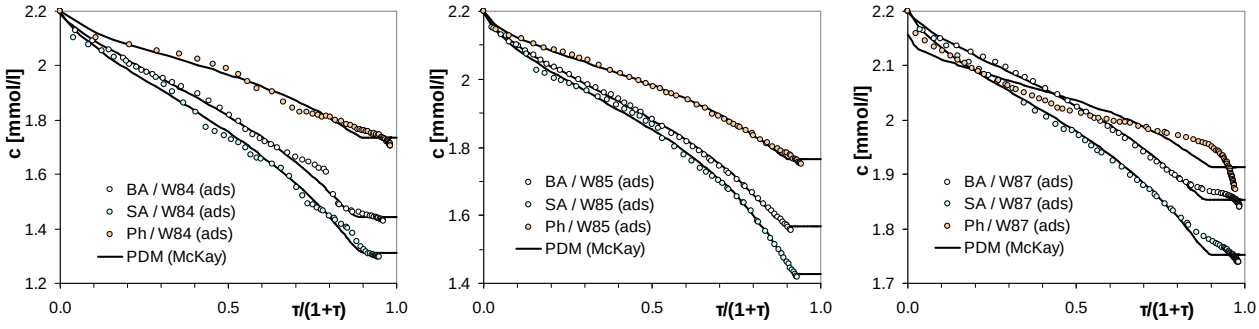

Fig. S12. Adsorption (pH=2) data of BA, SA and Ph on mesoporous carbons W84, W85, W87 - effect of adsorbate. in compact time plot, concentration vs. $\tau/(1+\tau)$, where $\tau = t/t_{0.5}$ is reduced time. Solid lines are PDM-optimizations.

Table S4. Effect of fitting assumptions on optimized parameters and fitting quality (PDM, McKay 1996). Units: c_o, c_{eq}, c_{05}, $SD(c)$ [mmol/l], $t_{0.5}$ [min].

BA	W84	W85	W87	W84	W85	W87	W84	W85	W87
fitted ->	c_{eq}, B, $t_{0.5}$			c_o, c_{eq}, B, $t_{0.5}$			c_o, c_{eq}, B, $t_{0.5}$, u_{eq}		
c_o	**2.2**	**2.2**	**2.2**	2.187	2.195	2.198	2.195	2.185	2.183
c_{eq}	1.441	1.567	1.853	1.442	1.568	1.853	1.443	1.561	1.85
u_{eq}	0.345	0.287	0.158	0.341	0.286	0.157	0.042	0.542	0.999
B	0.9499	0.9787	0.9619	0.9377	0.9747	0.9589	0.9664	0.9464	0.4323
t_{05}	19.6	40.3	20	20.3	41.1	20.3	20.1	42.7	21.6
1-R^2	0.00129	0.0008	0.00545	0.00122	0.00078	0.00545	0.00114	0.00062	0.00271
SD(c)	0.00964	0.00552	0.00737	0.00938	0.00547	0.00736	0.00906	0.00487	0.0052
c_{05}	1.821	1.884	2.027	1.815	1.881	2.026	1.819	1.873	2.016
SA	**W84**	**W85**	**W87**	**W84**	**W85**	**W87**	**W84**	**W85**	**W87**
fitted ->	c_{eq}, B, $t_{0.5}$			c_o, c_{eq}, B, $t_{0.5}$			c_o, c_{eq}, B, $t_{0.5}$, u_{eq}		
c_o	**2.2**	**2.2**	**2.2**	2.197	2.277	2.205	2.17	2.199	2.191
c_{eq}	1.312	1.426	1.753	1.312	1.426	1.753	1.298	1.423	1.743
u_{eq}	0.404	0.352	0.203	0.403	0.374	0.205	0.928	0.415	0.999
B	0.9599	0.9839	0.9782	0.9578	1.0156	0.9824	0.7667	0.9807	0.812
t_{05}	24	40.3	27.1	24.2	31.7	26.5	25.4	40.5	27.3
1-R^2	0.0057	0.00164	0.00536	0.0057	0.00164	0.00534	0.00277	0.00162	0.00079
SD(c)	0.02094	0.00949	0.01002	0.02093	0.00949	0.01	0.01459	0.00944	0.00384
c_{05}	1.756	1.813	1.976	1.754	1.851	1.979	1.734	1.811	1.967
Ph	**W84**	**W85**	**W87**	**W84**	**W85**	**W87**	**W84**	**W85**	**W87**
fitted ->	c_{eq}, B, $t_{0.5}$			c_o, c_{eq}, B, $t_{0.5}$			c_o, c_{eq}, B, $t_{0.5}$, u_{eq}		
c_o	**2.2**	**2.2**	**2.2**	2.2	2.199	2.158	2.181	2.175	2.184
c_{eq}	1.734	1.765	1.916	1.734	1.765	1.913	1.72	1.754	1.895
u_{eq}	0.212	0.198	0.129	0.212	0.197	0.113	0.999	0.857	0.993
B	0.9867	0.9942	1.0265	0.9867	0.9935	1.0017	0.7324	0.8768	1.0017
t_{05}	8.5	26.8	25.5	8.5	26.9	40.9	9.5	30.7	33.7
1-R^2	0.02381	0.00292	0.07926	0.02381	0.00292	0.07363	0.01108	0.0019	0.03129
SD(c)	0.01914	0.00713	0.02271	0.01914	0.00713	0.02189	0.01306	0.00576	0.01427
c_{05}	1.967	1.983	2.058	1.967	1.982	2.035	1.951	1.965	2.039

PDM halftimes, optimization: c_o, c_{eq}, B, $t_{0.5}$

t_{05} [min]	W84	W85	W87	geom.avg
BA	**20.3**	**41.1**	**20.3**	**25.68**
SA	**24.2**	**31.7**	**26.5**	**27.29**
Ph	**8.5**	**26.9**	**40.9**	**21.07**
geom.avg	**16.1**	**32.73**	**28.02**	**24.53**

gIKL/MOE plots

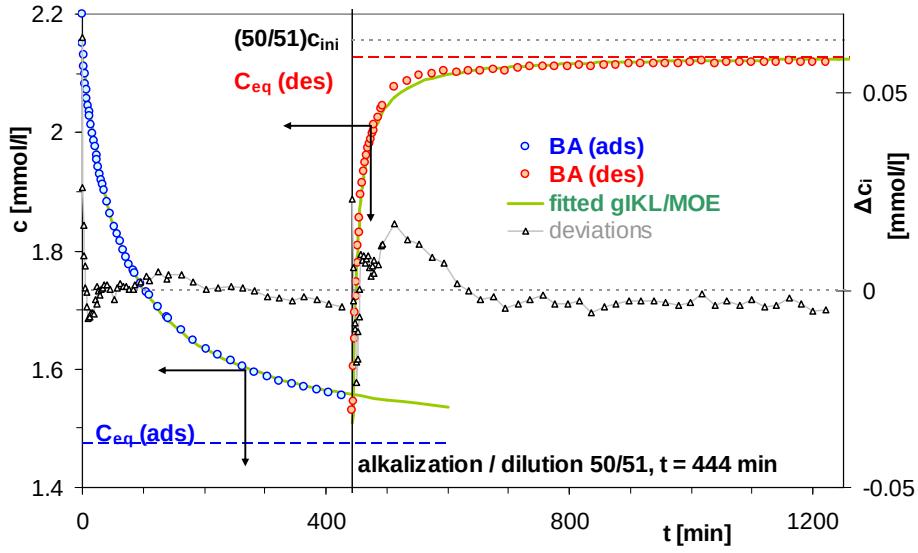

Fig. S13. Typical kinetic experiment: adsorption (pH=2) and desorption (pH=12) of benzoic acid (BA) on mesoporous carbon W85 compared with gIKL/MOE fitted lines in a common time scale.

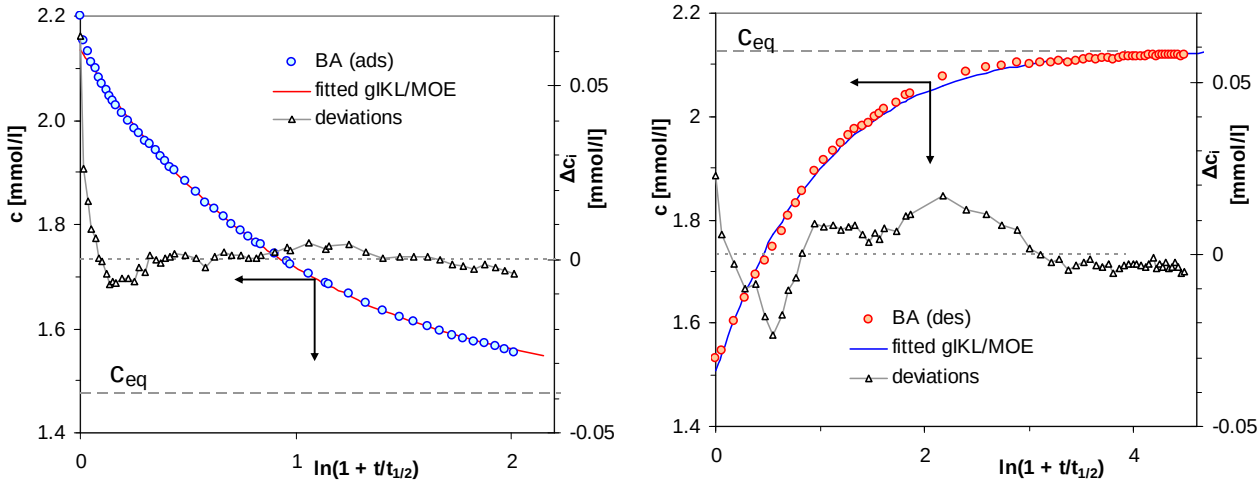

Fig. S14. Example of kinetic experiment: adsorption (pH=2, left) and desorption (pH=12, right) of benzoic acid (BA) on mesoporous carbon W85 compared with gIKL/MOE fitted lines (see Table) in a half-log time scale.

The following *compact time plots* are linear if f_2 (MOE) or f_L (gIKL) are equal to 1. However f_L=1 may be obtained only if equilibrium uptake u_{eq} = 1 and θ_{eq} = 1, i.e. for gIKL equilibrium concentration should be 0. For f_2<1 line is not linear (see Figs. 1,2 in the paper).

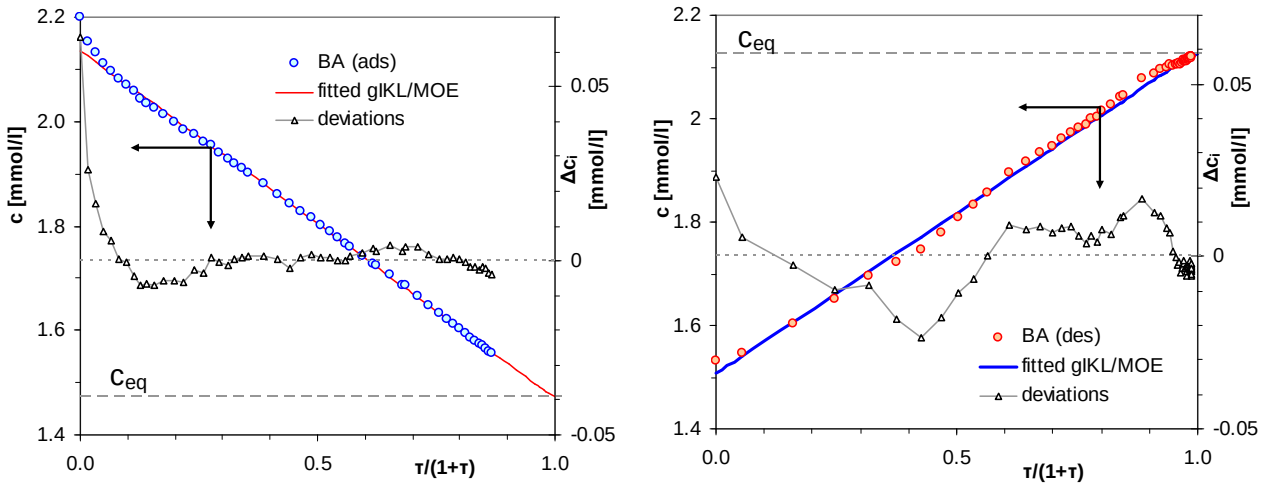

Fig. S15. Example of kinetic experiment: adsorption (pH=2, left) and desorption (pH=12, right) of benzoic acid (BA) on mesoporous carbon W85 compared with gIKL/MOE fitted lines (see Table 1) in a *compact time plot* linear for SO/PSO data ($\tau=t/t_{1/2}$ is the reduced time).

For all cases desorption halftimes were much smaller (1.5-8 times) than adsorption halftimes. With the exception of phenol, similar halftimes were obtained for W84 and W87 (both partly microporous). In the case of 6 (out of total 9) adsorption/desorption systems fitted with MOE parameters $f_{2,ads} > f_{2,des}$ as required by the IKL. However, as it was found these systems cannot be described to the pure Langmuir kinetics (IKL) – equilibrium isotherm is LF ($n<1$), as well as parameters $f_{2,ads}$ are too big to conform to the IKL f_{eq} (uptakes are 15-45% only, surface coverages are also <1) , i.e. do not fit the IKL. Moreover, kinetic parameters in some cases proved to be very susceptible to data deviations, also those resulting from changing fitting assumptions (e.g. $c_o=c_{ini}$, rejection of the 1st point for desorption – it is extrapolated from adsorption kinetic data). E.g. rate coefficient k_1 is specifically very susceptible to errors and fitting method especially if f2 is near 1– in contrast to kinetic halftime, which may be measured independently of the model and if experimental data is measured near equilibrium, should be practically constant independently on any other fitting peculiarity. Then for various fitting methods for gIKL/MOE/SOE as well as fractal-like f-MOE we should have constant approximately constant quantity $k_1/\ln(2-f_2)^{1/p}$ and k_2 (if $f_2=1$).

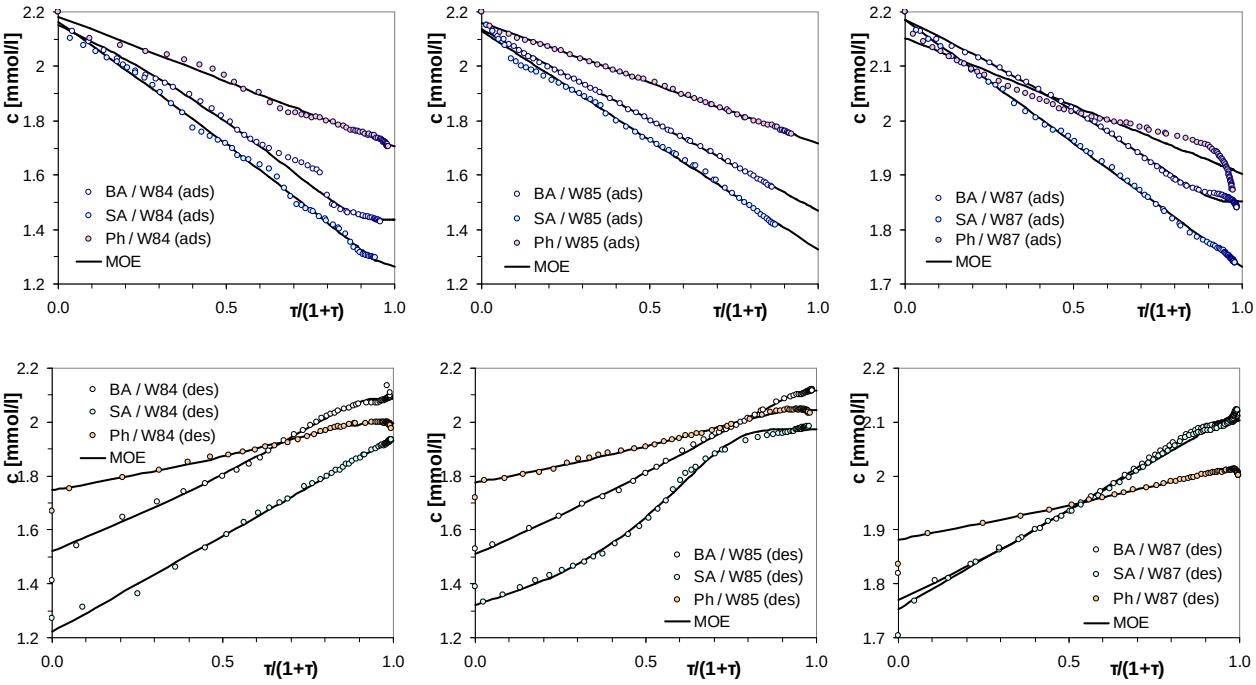

Fig. S16. Adsorption at *pH*=2 (top) and desorption at *pH*=12 (bottom) kinetics of BA, SA and Ph on mesoporous carbons at in compact time plot, concentration vs. $\tau/(1+\tau)$, where $\tau = t/t_{0.5}$ is reduced time. Solid lines are **MOE** (12,13) optimizations. Effect of adsorbate (single carbon – 3 adsorbates)

Table S5. Adsorption/desorption of BA, SA and Ph on mesoporous carbons. Optimized parameters and fitting quality (MOE, 12,13). Units: c_o, c_{eq}, c_{05}, $SD(c)$ [mmol/l], $t_{0.5}$ [min], k_1 [1/min]. Here, c_o is optimized value. For adsorption all points are used (1st point is experimental). For desorption, 1st point is removed from fitting, because it is extrapolated from adsorption data and corresponds to the sudden change of experimental conditions.

	ads	des	ads	des	ads	des
BA	**BA / W84**		**BA / W85**		**BA / W87**	
c_o	2.152	1.524	2.15	1.509	2.184	1.769
c_{eq}	1.437	2.088	1.479	2.115	1.851	2.104
f_2	0.523	0.668	1	0.842	0.698	0.737
k_1	0.0178	0.0434	0.0165	0.0162	0.0124	0.0285
$t_{0.5}$	21.9	6.6	60.7	9	21.3	8.2
$1\text{-}R^2$	0.00216	0.00422	0.00239	0.00114	0.00335	0.00477
$SD(c)$	0.01249	0.00851	0.00955	0.00518	0.00578	0.00488
c_{05}	1.794	1.806	1.814	1.812	2.018	1.937
	ads	des	ads	des	ads	des
SA	**SA / W84**		**SA / W85**		**SA / W87**	
c_o	2.162	1.223	2.131	1.323	2.185	1.754
c_{eq}	1.264	1.932	1.326	1.972	1.732	2.12
f_2	0.905	0.976	0.997	-1	0.999	0.999
k_1	0.0033	0.0046	0.00004	0.0568	0.00005	0.00007
$t_{0.5}$	27.6	5.1	61.6	19.3	29.2	9.9
$1\text{-}R^2$	0.00281	0.00252	0.00567	0.00278	0.00078	0.00323
$SD(c)$	0.01469	0.0074	0.01765	0.01134	0.00382	0.00476
c_{05}	1.713	1.577	1.728	1.647	1.959	1.937
	ads	des	ads	des	ads	des
Ph	**Ph / W84**		**Ph / W85**		**Ph / W87**	
c_o	2.183	1.748	2.161	1.776	2.152	1.882
c_{eq}	1.706	1.995	1.719	2.044	1.903	2.008
f_2	0.999	0.534	0.998	0.633	0.999	0.778
k_1	0.00011	0.0633	0.00006	0.0173	0.00002	0.0384
$t_{0.5}$	9.7	6	38.9	18	39	5.2
$1\text{-}R^2$	0.00993	0.00756	0.00266	0.0036	0.04997	0.01253
$SD(c)$	0.01236	0.00497	0.00681	0.00498	0.01803	0.00277
c_{05}	1.945	1.871	1.94	1.91	2.027	1.945

Table S7. Adsorption and desorption halftimes for kinetics fitted with MOE (12,13)

	ads					des			
t_{05} [min]	W84	W85	W87	geom. avg.	t_{05} [min]	W84	W85	W87	geom. avg.
BA	21.9	60.7	21.3	**30.48**	**BA**	6.6	9	8.2	**7.87**
SA	27.6	61.6	29.2	**36.75**	**SA**	5.1	19.3	9.9	**9.91**
Ph	9.7	38.9	39	**24.51**	**Ph**	6	18	5.2	**8.25**
geom. avg.	**18.03**	**52.59**	**28.95**	**30.17**	**geom. avg**	**5.87**	**14.62**	**7.5**	**8.63**

Comparison of adsorption and desorption halftimes shows, that generally (with the exception of Ph / W87), adsorption/desorption halftimes are the longest on W85 carbon possessing the largest contribution (25%) of micropores (also the smallest average pore sizes), the times are the shortest for W84 carbon (or comparable to W87) with almost no micropores. the largest pores and the largest surface (overall and external) area and pore volume.

For all carbons and adsorbates desorption is much faster then adsorption – one of the factors may be electrostatic repulsion of adsorbate anions from negatively charged surface. Moreover, strong affinity of neutral molecules makes them "stick" to the surface delaying the transport in pores during adsorption process. On the average, adsorption halftimes are 3.5 times as long as desorption ones.

Table S6. Ratio of adsorption and desorption halftimes for optimization with MOE (12,13)

carbon	W84	W85	W87	
adsorbate	**$t_{05,ads}$ / $t_{05,des}$**			**geom. avg**
BA	**3.32**	**6.74**	**2.6**	**3.9**
SA	**5.41**	**3.19**	**2.95**	**3.7**
Ph	**1.62**	**2.16**	**7.5**	**3.0**
geom.avg.	**3.07**	**3.6**	**3.86**	**3.5**

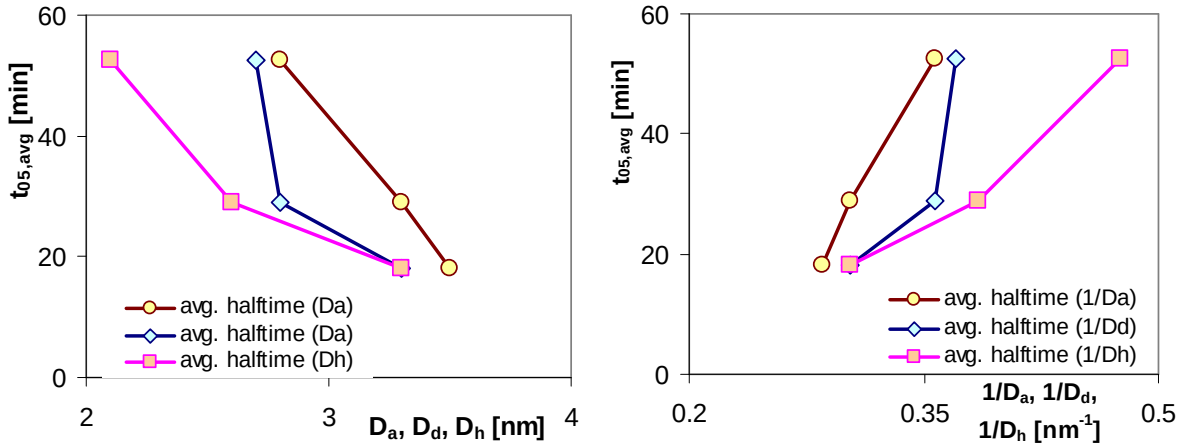

Fig. S17. Correlation of geometric-average halftimes (avg. for BA, SA and Ph) vs. pore sizes (a- adsorption, d-desorption, h-hydraulic) and their reciprocals.

Best correlation of average halftimes is for average mesopore size calculated from adsorption branch, D_a (see Table 2) (R^2=0.999) and only slightly worse for its reciprocal (R^2=0.994). It means that the average adsorption rate depends mainly on the mean width of mesopore adsorption channels, while local constrictions (evidenced by $D_d < D_a$) play much less important role). Similarly, adsorption halftimes are partially correlated to the "hydraulic" average pore size D_h (including micropores and mesopores) (correlation with $1/D_h^2$ gives R^2=0.987), which does not affect directly adsorption halftimes (easily accessible pores are filled first), however, (not shown here) its effects on times corresponding to near-equilibrium states (say, $t_{90\%}$) is much stronger.

Fractal-like MOE plots

Table S8. Adsorption/desorption of BA, SA and Ph on mesoporous carbons. Optimized parameters and fitting quality (fractal-like MOE, f-MOE 17,18). Units: c_o, c_{eq}, c_{05}, $SD(c)$ [mmol/l], $t_{0.5}$ [min], k_1 [1/min]. Here, c_o is optimized value. For adsorption all points are used (1st point is experimental). For desorption, 1st point is removed from fitting, because it is extrapolated from adsorption data and corresponds to the sudden change of experimental conditions.

	ads	des	ads	des	ads	des
BA	**BA / W84**		**BA / W85**		**BA / W87**	
c_o	2.185	1.466	2.199	1.534	2.2	1.796
c_{eq}	1.436	2.088	1.527	2.121	1.852	2.107
f_2	-1	-1	-0.731	0.997	-1	0.999
k_1	0.0558	0.2148	0.0217	0.0008	0.0579	0.0004
p	0.662	0.582	0.572	1.183	0.628	1.334
$t_{0.5}$	20.7	5.5	46.4	10	20.1	9.6
$1\text{-}R^2$	0.00078	0.00343	0.00017	0.00062	0.00299	0.00288
$SD(c)$	0.00752	0.00767	0.00252	0.00382	0.00545	0.00379
c_{05}	1.81	1.777	1.863	1.828	2.026	1.951
	ads	**des**	**ads**	**des**	**ads**	**des**
SA	**SA / W84**		**SA / W85**		**SA / W87**	
c_o	2.166	1.252	2.204	1.333	2.188	1.664
c_{eq}	1.227	1.933	1.36	1.971	1.738	2.114
f_2	0.999	1	-0.698	-1	0.955	-1
k_1	0.00005	0.00003	0.0205	0.05505	0.00141	0.2328
p	0.992	1.098	0.537	1.055	0.968	0.409
$t_{0.5}$	29.6	5.8	48.1	19.9	27.9	5.4
$1\text{-}R^2$	0.00282	0.00182	0.00152	0.00267	0.00075	0.00641
$SD(c)$	0.01474	0.00628	0.00914	0.01112	0.00376	0.00671
c_{05}	1.696	1.592	1.782	1.652	1.963	1.889
	ads	**des**	**ads**	**des**	**ads**	**des**
Ph	**Ph / W84**		**Ph / W85**		**Ph / W87**	
c_o	2.175	1.736	2.194	1.767	2.215	1.882
c_{eq}	1.71	1.995	1.749	2.044	1.812	2.008
f_2	0.999	-0.147	-1	0.277	0.978	0.753
k_1	0.00013	0.1264	0.04012	0.0283	0	0.0412
p	1.06	0.76	0.544	0.834	0.426	0.976
$t_{0.5}$	10	5.6	29.6	17.1	57.3	5.2
$1\text{-}R^2$	0.00972	0.00704	0.00077	0.00335	0.01875	0.01252
$SD(c)$	0.01223	0.00479	0.00366	0.0048	0.01105	0.00277
c_{05}	1.943	1.865	1.972	1.906	2.014	1.945

Comparison of indetermination coefficients for MOE

MOE	**ads**	**des**	**ads**	**des**	**ads**	**des**	
1-R2	W84	W84	W85	W85	W87	W87	**geom.avg.**
BA	0.00216	0.00422	0.00239	0.00114	0.00335	0.00477	0.002711
SA	0.00281	0.00252	0.00567	0.00278	0.00078	0.00323	0.00256
Ph	0.00993	0.00756	0.00266	0.0036	0.04997	0.01253	0.008754
geom.avg.	0.003921	0.004316	0.003303	0.002251	0.005073	0.00578	0.003931

Comparison of indetermination coefficients for fractal-like MOE

f-MOE	**ads**	**des**	**ads**	**des**	**ads**	**des**	
1-R2	W84	W84	W85	W85	W87	W87	**geom.avg.**
BA	0.00078	0.00343	0.00017	0.00062	0.00299	0.00288	0.001159
SA	0.00282	0.00182	0.00152	0.00267	0.00075	0.00322	0.001921
Ph	0.00972	0.00704	0.00077	0.00335	0.01875	0.01252	0.005883
geom.avg.	0.002775	0.003529	0.000584	0.00177	0.003477	0.004878	0.002358

Table S9. Ratio of (1-R^2) obtained by fractal-like MOE (17,18) and MOE (12,13) optimizations for BA, SA and Ph adsorption on W84, W85 and W87 carbons. Small values denote high improvement by using f-MOE. Geometric mean values for adsorbates (right) and carbons (ads/des experiments), for adsorption or desorption curves and for all experiments.

(1-R^2) ratio f-MOE / MOE:	ads	des	ads	des	ads	des	Geometric means
carbon	W84	W84	W85	W85	W87	W87	
BA	0.361	0.813	0.071	0.544	0.893	0.604	0.428
SA	1.004	0.722	0.268	0.96	0.962	0.997	0.751
Ph	0.979	0.931	0.289	0.931	0.375	0.999	0.672
Geometric means	0.708	0.818	0.177	0.786	0.685	0.844	0.6
Geometric means	0.761		0.373		0.761		
Geometric means	0.441	0.816					

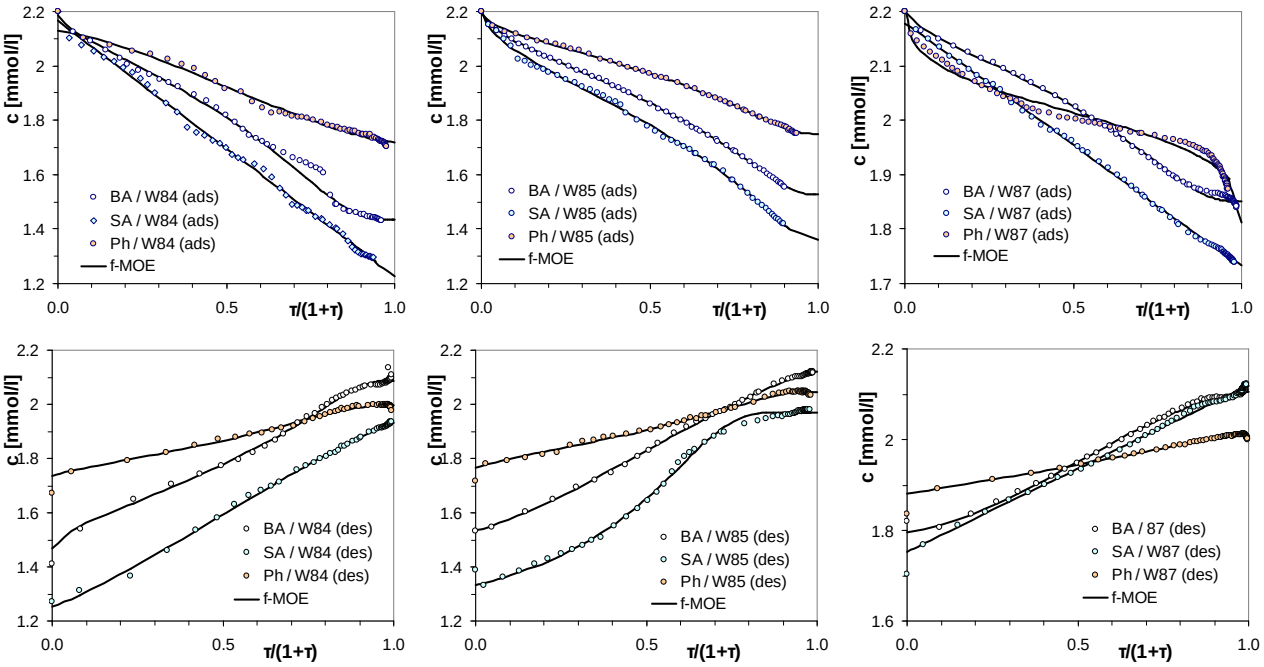

Fig. S18. Adsorption at *pH*=2 (top) and desorption at *pH*=12 (bottom) kinetics of BA, SA and Ph on mesoporous carbons at in compact time plot, concentration vs. τ/(1+τ), where $\tau = t/t_{0.5}$ is reduced time. Solid lines correspond to – **fractal-like MOE** (17,18) optimizations. Effect of adsorbate (single carbon – 3 adsorbates)

We may see (Tables S8,9), that in some cases using f-MOE did not improve fitting, however, in some cases (with strong deviations from MOE near beginning or end of kinetic curves) high improvements are noted. On average, 1-R2 were smaller by 40% (1-R^2 ratio for f-MOE / MOE ~ 0.6). The highest improvements were noted for adsorption and desorption on W85 characterized by the highest adsorbed amounts. We may attribute this improvement to the more precise data, where deviations from model are better visible. For W84 and W87 this improvement is still present, but not so pronounced.

Comparison of adsorption and desorption halftimes shows, that generally (with the exception of Ph / W87), adsorption/desorption halftimes are the longest on W85 carbon possessing the largest contribution (25%) of micropores (also the smallest average pore sizes), the times are the shortest

for W84 carbon (or comparable to W87) with almost no micropores. the largest pores and the largest surface (overall and external) area and pore volume.

Table S10. Adsorption and desorption halftimes for kinetics fitted with f-MOE (17,18)

	ads				des			
t_{05} [min]	W84	W85	W87	geom. avg	t_{05} [min]	W84	W85	W87	geom. avg
BA	20.7	46.4	20.1	26.83	BA	5.5	10	9.6	8.08
SA	29.6	48.1	27.9	34.12	SA	5.8	19.9	9.8	10.42
Ph	10	29.6	57.3	25.69	Ph	5.6	17.1	5.2	7.93
geom. avg	18.3	40.43	31.79	28.65	geom. avg	5.63	15.04	7.88	8.74

For all carbons and adsorbates desorption is much faster then adsorption – one of the factors may be electrostatic repulsion of adsorbate anions from negatively charged surface. Moreover, strong affinity of neutral molecules makes them "stick" to the surface delaying the transport in pores during adsorption process. On the average, adsorption halftimes for fractal-like MOE are 3.3 times as long as desorption ones, i.e. almost the same as 3.5 for MOE (12,13). Similarly as for MOE, such differences are apparently the largest for phenol. However, if we remove from comparison Ph / W87 (adsorption curve for Ph / W87 differs from all other systems independent on the analysis type) this ratio becomes the smallest for phenol (~2), whereas for BA and SA it is almost the same.

Table S11. Ratio of adsorption and desorption halftimes for optimization with fractal-like MOE (17,18)

carbon	W84	W85	W87	
adsorbate	$t_{05,ads}$ / $t_{05,des}$			geom. avg
BA	3.76	4.64	2.09	3.3
SA	5.1	2.42	2.85	3.3
Ph	1.79	1.73	11.02	3.2
geom avg	3.25	2.69	4.03	3.3

Some comments on gIKL/MOE/SO fitting:

Optimized values of $t_{1/2}$ were approximately linearly dependent on f_2.

However, 1-R^2, $SD(c)$ and $\log(\sum(c_i - c(t_i))^2)$ were approximately quadratically dependent of f_2 and almost linearly dependent on $(f_2 - f_{2,opt})^2/(1+f_2)^2$ (with the same slope below and above $f_{2,opt}$ for desorption). This kind of relatively weak relation means that very close to the optimum various solutions are almost equivalent (e.g. f_2=0.998 and 1 were almost undistinguishable).